

Methods to calculate scalar two-loop vertex diagrams

J. FLEISCHER

Fakultät für Physik, Universität Bielefeld
D-33615 Bielefeld, Germany
E-mail: fleischer@physik.uni-bielefeld.de.

M. TENTYUKOV*

Joint Institute for Nuclear Research,
141980 Dubna, Moscow Region, Russian Federation.
E-mail: tentukov@thsun1.jinr.dubna.su

Abstract

We present a review of the Bielefeld-Dubna activities on multiloop calculations.

In the first contribution of the above authors in these proceedings, we have introduced our system for the automation of evaluation of Feynman diagrams, called DIANA (DIagram ANALyser). In this contribution methods for the evaluation of scalar two-loop integrals will be discussed.

1 Expansion of three-point functions in terms of external momenta squared

Taylor series expansions in terms of one external momentum squared, q^2 say, were considered in [1], Padé approximants were introduced in [2] and in Ref. [3] it was demonstrated that this approach can be used to calculate Feynman diagrams on their cut by analytic continuation. The Taylor coefficients are expressed in terms of “bubble diagrams”, i.e. diagrams with external momenta equal zero, which makes their evaluation relatively easy. In the case under consideration we have two independent external momenta in $d = 4 - 2\varepsilon$ dimensions. The general expansion of (any loop) scalar 3-point function with its momentum space representation $C(p_1, p_2)$ can be written as

$$C(p_1, p_2) = \sum_{l,m,n=0}^{\infty} a_{lmn} (p_1^2)^l (p_2^2)^m (p_1 p_2)^n \quad (1)$$

where the coefficients a_{lmn} are to be determined from the given diagram.

For many applications it suffices to confine to the case $p_1^2 = p_2^2 = 0$, which is e.g. physically realized in the case of the Higgs decay into two photons ($H \rightarrow \gamma\gamma$) with p_1 and p_2 the momenta of the photons. In this case only the coefficients a_{00n} are needed.

In the two-loop case we consider the scalar integral ($k_3 = k_1 - k_2$, see also Fig. 1)

$$C(m_1, \dots, m_6; p_1, p_2) = \frac{1}{(i\pi^2)^2} \int \frac{d^4 k_1 d^4 k_2}{((k_1 + p_1)^2 - m_1^2)((k_1 + p_2)^2 - m_2^2)((k_2 + p_1)^2 - m_3^2)((k_2 + p_2)^2 - m_4^2)(k_2^2 - m_5^2)(k_3^2 - m_6^2)}. \quad (2)$$

k_t in line 4 (with mass m_4) depends on the topology: for the *planar* diagram we have $k_t = k_2$ while for the *non-planar* we have $k_t = k_3$.

With obvious abbreviations for the scalar propagators: c_i the i^{th} scalar propagator of (2) with $p_1 = p_2 = 0$, we can quite generally write for the n^{th} Taylor coefficient [4]:

$$(i\pi^2)^2 a_{00n} = \frac{2^n}{n+1} \int d^4 k_1 d^4 k_2 F_n \cdot \frac{1}{c_1 c_2 c_3 c_4 c_5 c_6}. \quad (3)$$

* Supported by Bundesministerium für Forschung und Technologie under PH/05-7BI92P 9.

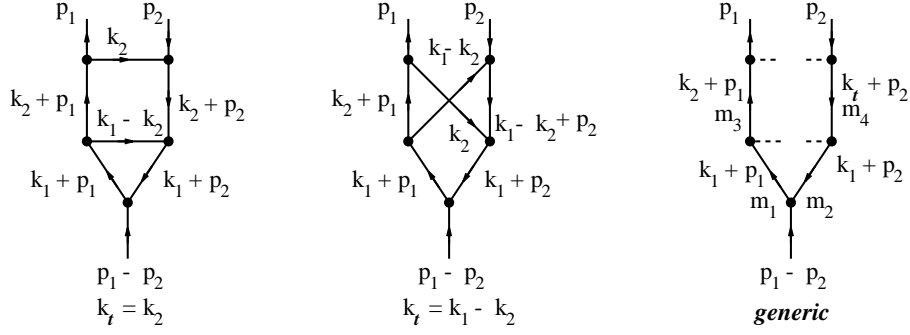


Figure 1: Planar and non-planar scalar vertex diagrams and their kinematics

The numerator F_n can be written as

$$F_n = \sum_{\nu=0}^n c_1^{-(n-\nu)} c_3^{-\nu} \sum_{\nu'=0}^n c_2^{-(n-\nu')} c_4^{-\nu'} \cdot A_{\nu\nu'}^n(k_1, k_2, k_t). \quad (4)$$

For the *planar* diagram ($k_t = k_2$) we have

$$A_{\nu\nu'}^n(k_1, k_2) = \sum_{\mu=\max(0, \nu+\nu'-n)}^{\lfloor \frac{\nu+\nu'}{2} \rfloor} a_{\nu\nu'}^{n\mu}(k_1^2)^{n-(\nu+\nu')+\mu} (k_2^2)^\mu (k_1 k_2)^{\nu+\nu'-2\mu}. \quad (5)$$

The coefficients $a_{\nu\nu'}^{n\mu}$ are mass independent and have been calculated with FORM up to order ε^2 ($d = 4 - 2\varepsilon$) and stored for the first 30 Taylor coefficients, i.e. they are given in terms of rational numbers.

Finally all remaining integrals can be reduced by recursion [5] to bubble-integrals of the type

$$V_{\alpha\beta\gamma}(\{m\}) = \int \frac{d^d k_1 d^d k_2}{(k_1^2 - m_1^2)^\alpha (k_2^2 - m_2^2)^\beta ((k_1 - k_2)^2 - m_3^2)^\gamma}, \quad (6)$$

or to factorizing one-loop integrals. The genuine two-loop bubble integrals are reduced by means of recurrence relations to $V_{111}(\{m\})$. This can be done numerically for the arbitrary mass case or also analytically for special cases like e.g. only one non-zero mass. For details see [4],[5]. To perform the recursion numerically, it is important to use the multiple precision FORTRAN by D.Bailey ([6]) since tremendous cancellations occur in this case.

We have presented one approach for the calculation of the Taylor expansion of Feynman diagrams in some detail, others were worked out in Refs. [7],[8]. The latter one is particularly suited for programming in terms of a formulae manipulating language like FORM.

2 The method of analytic continuation

We assume the Taylor expansion of a scalar diagram to be given in the form $C(p_1, p_2, \dots) = \sum_{m=0}^{\infty} a_m y^m \equiv f(y)$ and the function on the r.h.s. has a cut for $y \geq y_0$. If the diagram has a threshold at $4m^2$ it is suggestive to introduce $y = q^2/4m^2$ with $q^2 = (p_1 - p_2)^2$ as adequate variable with $y_0 = 1$.

The method of evaluation of the original series consists in a first step in a conformal mapping of the cut plane into the unit circle and secondly the reexpansion of the function under consideration into a power series w.r.t. the new conformal variable. A variable often used is

$$\omega = \frac{1 - \sqrt{1 - y/y_0}}{1 + \sqrt{1 - y/y_0}}. \quad (7)$$

By this conformal transformation, the y -plane, cut from y_0 to $+\infty$, is mapped into the unit circle (see Fig.2) and the cut itself is mapped on its boundary, the upper semicircle corresponding to the upper side

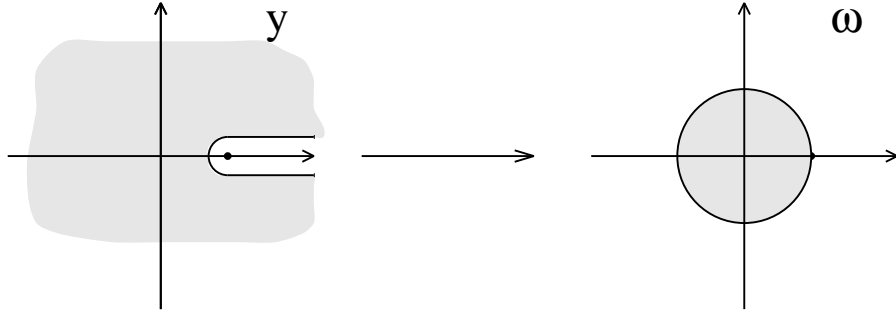


Figure 2: Conformal mapping of the $y = q^2/4m_t^2$ -complex plane into the ω -plane.

of the cut. The origin goes into the point $\omega = 0$.

After conformal transformation it is suggestive to improve the convergence of the new series w.r.t. ω by applying the Padé method [9],[10]. A convenient technique for the evaluation of Padé approximations is the ε -algorithm of [9] which allows one to evaluate the Padé approximants recursively.

Many interesting examples for the efficiency of this method have been worked out in the meantime and we refer to the literatur for massive diagrams to [3], [12], [13] e.g.

3 Two-loop vertex diagrams with zero thresholds

Concerning the vertex diagrams, there are many different topologies contributing to a 3-point function in the SM. For our purpose of demonstrating the method, we confine ourselves to the planar case shown in Fig. 3a. Fig. 3c,d presents infrared divergent diagrams.

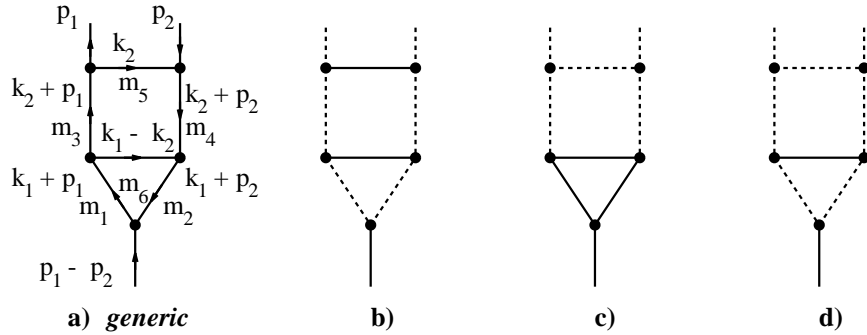


Figure 3: Planar diagrams with zero thresholds. a)—generic; b)—IR finite diagram; c),d)—IR divergent diagrams.

As a typical (and very complicated case) we consider here Fig. 3b with equal non-zero masses [14]. There are two massless cuts so that we shall have the double logarithm in the expansion. After summing up four contributions we see that the double and single poles in ε cancel as well as the scale parameter μ , with the result ($x = q^2/M^2$)

$$\begin{aligned}
 F(q^2, M^2) &= \frac{1}{M^4} \sum_{n=0}^{\infty} \sum_{j=0}^2 f_{jn} \ln^j(-x) x^n \\
 &\equiv \frac{1}{M^4} \{ f_0(x) + f_1(x) \ln(-x) + f_2(x) \ln^2(-x) \}, \tag{8}
 \end{aligned}$$

where the f_{jn} are now given in terms of rational numbers and $\zeta(2)$. $f_2(x)$ can be summed analytically,

Table 1: Results for timelike q^2 for diagram 3b.

q^2/M^2	[12/12]		[15/15]	
	Re	Im	Re	Im
0.05	+2.948516245	20.938528	+2.948516245	20.938528
0.1	-1.108116127	16.04132127	-1.108116127	16.04132127
0.5	-4.820692281	5.066080015	-4.820692281	5.066080015
1.0	-3.890154	1.67549787	-3.890156	1.67549788
1.5	-2.904588	0.42979	-2.904581	0.429778
2.0	-2.18294	-0.06976	-2.182981	-0.069728
10.0	-0.191	-0.208	-0.194	-0.215

yielding

$$f_2(x) = (\ln|1+x| - i\pi\theta(1+x))^2/x^2. \quad (9)$$

Thus, we have to Padé approximate f_0 and f_1 only. Close to the second threshold at $q^2 = M^2$ the convergence is indeed excellent (see Table 1) [14]. It should be noted that for the physical application we have in mind, i.e. $Z \rightarrow b\bar{b}$, this is just the case of interest. It is worthwhile to note the sharp increase for low q^2 due to $\ln^2(-q^2/M^2)$.

The infrared divergent diagrams (Fig. 3c,d) have been successfully considered in [15].

4 The Differential Equation Method

We saw that to obtain the expansion of a diagram one has to go through a rather cumbersome machinery. The more coefficients are asked for, the more efforts and machine resources are required. Thus it is very desirable to have analytic expressions for expansion coefficients whenever possible. This can be done with the aid of the Differential Equation Method (DEM) [16] if only one non-zero mass occurs. The DEM allows one to get results for massive diagrams by reducing the problem to diagrams with simpler structure.

Let us introduce a graphical notation for the scalar propagators (in euclidean space-time)

$$\frac{1}{(q^2)^\alpha} = \begin{array}{c} \alpha \\ \cdots \cdots \cdots \\ \bullet \end{array}, \quad \frac{1}{(q^2 + m^2)^\alpha} = \begin{array}{c} \alpha \\ \bullet \\ \text{---} \\ m^2 \end{array}$$

α and m refer to the index and mass of a line. Then one can derive the following recurrence relation for a massive triangle [16]

$$\begin{aligned} & \begin{array}{c} \alpha_2 \quad \alpha_3 \\ \triangle \\ \alpha_1 \end{array} (D - 2\alpha_1 - \alpha_2 - \alpha_3) = -2m_1^2 \alpha_1 \begin{array}{c} \alpha_2 \quad \alpha_3 \\ \triangle \\ \alpha_1+1 \end{array} \\ & + \alpha_2 \left(\begin{array}{c} \alpha_2+1 \quad \alpha_3 \\ \triangle \\ \alpha_1-1 \end{array} - \begin{array}{c} \alpha_2+1 \quad \alpha_3 \\ \triangle \\ \alpha_1 \end{array} - (m_1^2 + m_2^2) \begin{array}{c} \alpha_2+1 \quad \alpha_3 \\ \triangle \\ \alpha_1 \end{array} \right) + (\alpha_2 \leftrightarrow \alpha_3) \end{aligned}$$

along with some other graphical relations (see details in [16]).

Using this technique we analysed in [17] the class of 3-point two-loop massive graphs. As an example for the diagram of Fig.3c we get

$$(D-4)J_{5c} = 2 \begin{array}{c} \text{---} \\ \diagup \quad \diagdown \\ \text{---} \\ \bigcirc \\ \text{---} \\ 2 \end{array} - 2 \begin{array}{c} \text{---} \\ \diagup \quad \diagdown \\ \text{---} \\ \diagdown \quad \diagup \\ \text{---} \\ 2 \end{array} - 4m^2 \begin{array}{c} \text{---} \\ \diagup \quad \diagdown \\ \text{---} \\ \diagdown \quad \diagup \\ \text{---} \\ 2 \end{array} - 2m^2 \begin{array}{c} \text{---} \\ \diagup \quad \diagdown \\ \text{---} \\ \diagdown \quad \diagup \\ \text{---} \\ 2 \end{array} \quad (10)$$

In the r.h.s. of (10) the last two terms can be combined, resulting in dJ/dm^2 while for the second term we proceed in turn as

$$(D-4) \text{ (triangle with dashed top)} = \text{(triangle with curved top)} + \text{(triangle with dashed top and curved line)} - \text{(triangle with dashed top and two curved lines)} \quad (11)$$

Thus we are left with simple diagrams (these can be done completely by Feynman parameters) and the derivative of the initial diagram w.r.t. m^2 . The solution of the corresponding differential equation in terms of a series obtained from an integral representation reads

$$J_{5c} = -\frac{\Gamma^2(1+\varepsilon)}{(q^2)^2(m^2)^{2\varepsilon}} \sum_{n=1}^{\infty} \frac{(-x)^n \Gamma^2(n)}{\Gamma(2n+1)} \left[\frac{1}{\varepsilon^2} - \frac{1}{\varepsilon} \left(\ln(x) + S_1(n-1) \right) - \frac{3}{2} S_2(n-1) \right. \\ \left. - \frac{15}{2} S_1^2(n-1) + 4S_1(n-1)S_1(2n) - \zeta(2) - \ln(x)S_1(n-1) + \frac{1}{2} \ln^2(x) \right],$$

where

$$S_l(n) = \sum_1^n \frac{1}{k^l}$$

A similar formula was obtained for the diagram of Fig.3d (see [17]).

5 Large mass expansion versus small momentum expansion

If there are two or more different masses involved the coefficients a_{lmn} in (1) are not just numbers any more but complicated functions of mass ratios. If one of the masses is large, e.g. if the diagram contains a top, one can try to perform a large mass (LM, see [18]) expansion rather than a small momentum expansion.

Let us consider the diagram with $m_1 = m_2 = m_{top}$, $m_3 = m_4 = m_5 = 0$ and $m_6 = m_W$ (see e.g. [19]). There are again three subgraphs to be expanded. By direct evaluation we find that there are induced poles of the order $1/\varepsilon^3$ in subgraphs while in the sum they cancel which serves as a good check. For this particular diagram the result of the LM expansion looks like

$$\text{dia} = \sum_{n=-1}^{\infty} A_n = \left(b_n^{(0)} + b_n^{(1)}L + b_n^{(2)}L^2 + b_n^{(3)}L^3 \right) \left(\frac{1}{m_{top}^2} \right)^n \quad (12)$$

with $L = \log(m_{top}^2/\mu^2)$ and $b_n^{(i)}$'s being known functions of q^2 , m_W^2 and μ^2 .

The considered diagram is evaluated numerically at $\mu = m_{top} = 180$, $m_W = 80$, $q^2 = 90^2$. It turns out that also here again it is extremely useful to improve the convergence of the LM expansions by applying Padé approximants. Up to a normalization factor $\frac{1}{16\pi^2} \frac{1}{m_{top}^4}$ we obtain for the diagram (-9.996,17.9527), taking into account terms up to $n=10$ in (12). The Taylor expansion with 8 coefficients yields a precision of appr. 10 decimals the reason for which is that q^2 is far below the threshold. The advantage of the LM expansion, however, is that it is easier to program and for many purposes the achieved precision is high enough.

6 Conclusion

Any involved calculation in field theory necessarily consists of two parts: 1) automatic generation of Feynman diagrams and source codes and 2) techniques of evaluating scalar Feynman diagrams. In our contributions we presented both and the methods have a standard that soon important applications can be considered.

References

- [1] A.I. Davydychev and J.B. Tausk, Nucl. Phys., **B397** (1993) 123.
- [2] D.J. Broadhurst, J. Fleischer and O.V. Tarasov, Z.Phys., **C 60** (1993) 287.
- [3] J. Fleischer and O.V. Tarasov, Z.Phys., **C 64** (1994) 413.
- [4] J. Fleischer and O.V. Tarasov, in proceedings of the ZiF conference on Computer Algebra in Science and Engineering, Bielefeld, 28-31 August 1994, World Scientific 1995, J. Fleischer, J. Grabmeier, F.W.Hehl and W.Küchlin editors.
- [5] K.G. Chetyrkin and F.V. Tkachov, Nucl. Phys. **B192** (1981) 159; F.V. Tkachov, Phys. Lett. **100B** (1981) 65.
- [6] D.H. Bailey, *ACM Transactions on Mathematical Software*, 19 (1993) 288.
- [7] A.I. Davydychev and J.B. Tausk, Nucl. Phys., **B465** (1996) 507.
- [8] O.V. Tarasov, Nucl. Phys., **B480** (1996) 397.
- [9] D. Shanks, J. Math. and Phys. (Cambridge, Mass.) **34** (1955) 1; P. Wynn, Math. Comp. **15** (1961) 151; G.A. Baker, P. Graves-Morris, Padé approximants, in Encyl.of math.and its appl., Vol. **13, 14**, pp Addison-Wesley (1981).
- [10] G.A. Baker, Jr., J.L. Gammel and J.G. Wills, J.Math.Anal.Appl., **2** (1961) 405; G.A. Baker, Jr., Essentials of Padé Approximants, pp Academic Press (1975).
- [11] A. Djouadi, M. Spira and P.M. Zerwas, Phys. Lett., **B311** (1993) 255.
- [12] J.Fleischer, Proceedings of Fourth International Workshop on Software Engineering, Artificial Intelligence and Expert System for High Energy and Nuclear Physics (Pisa, Italy, April 3-8, 1995), p 103.
- [13] J. Fleischer and O.V. Tarasov, Proceedings of the 1996 Zeuthen Workshop on Elementary Particle Theory : QCD and QED in higher Orders (Rheinsberg, Germany, April 21 - 26, 1996).
- [14] J. Fleischer, V. Smirnov and O.V. Tarasov, Z. Phys. **C74** (1997) 379.
- [15] J. Fleischer et al., hep-ph/9704353, to be published in Z. Phys. **C**.
- [16] A.V. Kotikov, Phys.Lett. **B254** (1991) 185; ibid. **B259** (1991) 314; ibid. **B267** (1991) 123.
- [17] J. Fleischer, A.V. Kotikov and O.L. Veretin, Bielefeld preprint BI-TP-97/26, Phys.Lett. in print; (hep-ph/9707492).
- [18] F.V. Tkachov, Preprint INR P-0332, Moscow (1983); P-0358, Moscow (1984); K.G. Chetyrkin, Teor. Math. Phys. 75 (1988), 26; ibid 76 (1988), 207; Preprint, MPI-PAE/PTh-13/91, Munich (1991); V.A. Smirnov, Comm. Math. Phys. 134 (1990), 109; *Renormalization and asymptotic expansions* (Birkhäuser, Basel, 1991).
- [19] J. Fleischer, M. Kalmykov and O. Veretin, *Large Mass Expansion versus Small Momentum Expansion of Feynman Diagrams*, Bielefeld preprint BI-TP-97/43, in preparation.